Air Plasma Key Parameters for Electromagnetic Wave Propagation at and Out of Thermal Equilibrium: Applications to Electromagnetic Compatibility

P. Andre [1], G. Faure [1], A. Mahfouf [1], and S. Lalléchère [2]

[1] LPC, UMR CNRS 6533
Université Clermont Auvergne, F-63000 CLERMONT-FERRAND, France
{pascal.andre}/{geraldine.faure}@uca.fr, mahfoufphysique@gmail.com

[2] Institut Pascal, UMR CNRS 6602
Université Clermont Auvergne, CNRS, BP 10448, F-63000 Clermont-Ferrand, France
sebastien.lallechere@uca.fr

Abstract ─ This article addresses the importance of accurate characterization of plasma parameters for electromagnetic compatibility (EMC) purposes. Most of EMC issues involving plasma materials are obviously multi-physics problems (linking chemical, mechanical, thermal and electromagnetic wondering) with deep interactions. One of the main objectives of this paper is to establish the theoretical effect of thermal non-equilibrium of the plasma on electromagnetic wave propagation. This will be characterized throughout plasma key parameters (including complex permittivity). Numerical simulations based upon Finite Integral Technique (FIT) will demonstrate the EMC interest of this methodology for shielding purposes and general air plasma.

Index Terms ─ Dielectric parameters, electromagnetic compatibility, electromagnetic propagation, plasmas, plasma modelling, thermal equilibrium.

I. INTRODUCTION

The interaction of an electromagnetic wave with an air plasma can be found in many applications as the Inductively Coupled Plasmas (ICPs) used for spectrochemical analyses [1], in plasmas analyses (the electromagnetic wave can be used to measure the electronic concentration) [2], in the dielectric barrier discharge that have promised applications as the regeneration of Diesel particle or the Gas Insulated System (GIS) [3, 4], in telecommunication applications [5] for instance.

Intentional or non-intentional plasma generations imply highly multi-physics studies involving chemistry, thermic, physics and of course electromagnetics to properly characterize electromagnetic (EM) fields. Previous studies [6-7] have demonstrated that a better understanding is needed to avoid microwave breakdowns and so improve shielding effectiveness (SE) of enclosures embedded with slots and equipment under test. Some current electromagnetic compatibility (EMC) issues require an accurate assessment of materials EM properties in various configurations: for instance damaging of aeronautical systems (wires, antennas) due to lightning, spacecraft re-entry (radio frequency, RF, plasma generation).

The electromagnetic wave can produce useful plasma as in ICPs, can go through existing plasma as in plasma analyses or in telecommunication applications, or can produce an electrical breakdown.

Due to their higher mobility the electrons can reach a temperature (T_e) higher than the one of the other chemical species (T_h). The temperatures have been measured in several applications as discharges with liquid non-metallic electrodes [8], have been evaluated from the applied electrical field [9], or have been taken into account in modelling [10], circuit breakers, arc tracking, RADAR applications.

Modelling of electromagnetic waves in interaction with a material requires available physical properties of the material as dielectric permittivity [11]. The dielectric permittivity depends greatly on thermodynamic state and in the case of plasma on temperatures (T_e, T_h). It is also to be noticed that the dual interaction electromagnetic (EM) field/dielectric permittivity and dielectric permittivity/EM field has been recently explored in [5] regarding electrostatic fields and low permittivity barriers. The latter parametric study highlighted the importance of dielectric slab properties (e.g., permittivity, width, EM field's magnitude). It provided optimized characteristics (e.g., barrier width) with regards to the value needed for breakdown voltage.

In a previous work [12], we have shown that thermal non-equilibrium plays a major influence on argon plasma properties as London and Kelvin lengths. Consequently magnetic field is absorbed by the material in a direct way depending on the thermal state of the plasma.

Submitted On: June 9, 2016
Accepted On: November 4, 2018

The effect of thermal disequilibrium on the plasma properties (London and Kelvin lengths, dielectric permittivity) depends on chemical composition. To determine the concentrations of the chemical species concentration versus heavy species temperatures, we use the Gibbs free energy method [13]. We need to know for each chemical species the chemical potential as describe in [14]. We assume a dry air initial composition that is to say 80% of nitrogen N_2 and 20% of oxygen O_2 in molar percentage. We take 9 monatomic chemical species (N, N^+, N^{++}, N^{+++}, O, O^-, O^+, O^{++}, O^{+++}), 9 diatomic chemical species (N_2, N_2^-, N_2^+, NO, NO^-, NO^+, O_2, O_2^-, O_2^+) and 11 polyatomic species (N_2O, N_2O_3, N_2O_4, N_2O_5, N_2O^+, N_3, NO_2, NO_2^-, NO_3, O_3, NO_3^-) and electrons into account.

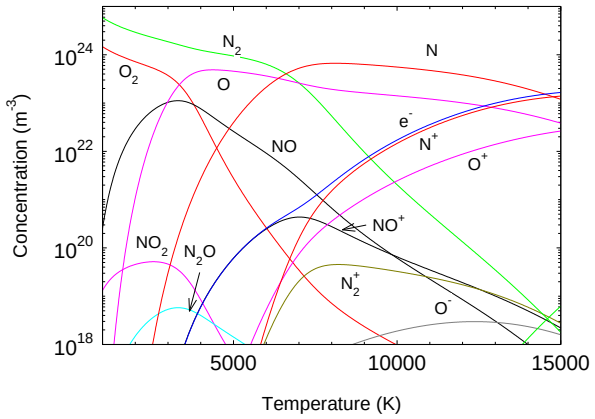

Fig. 1. Air composition at atmospheric pressure at thermal equilibrium.

In Figs. 1 and 2, we show the concentration evolution of the considered chemical species versus heavy species temperature (T_h) at thermal equilibrium and out of thermal equilibrium ($\theta = {T_e}/{T_h}$) for air plasma at atmospheric pressure. These figures clearly depict the high differences existing between concentrations of heavy species and electrons at and out of thermal equilibrium for air plasma at atmospheric pressure. In the latter figures, we can observe that ionisation appears at lower heavy species temperature when the thermal non equilibrium ratio θ increases for a given heavy species temperature T_h. So the electrons appear at lower temperature and have certainly an influence on physical parameters. Consequently, one of the main purposes of the paper is to study the influence of the thermal disequilibrium on the key physical parameters needed to EM simulation.

This article is organized as follows: in Section II we describe the theoretical methodology and the key parameters (plasma frequency, electron collision frequency, permittivity) for EM simulations are evaluated in an air plasma at atmospheric pressure at thermal equilibrium and out of thermal equilibrium. In Section III we study the EM field propagation through the plasma, and an EMC illustrative example is proposed. The contribution ends with Section IV constituting a conclusion with some prospects.

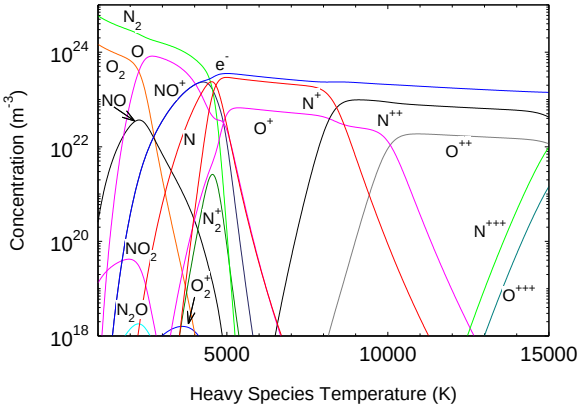

Fig. 2. Air composition at atmospheric pressure out of thermal equilibrium $\theta = T_e/T_h = 3$.

II. PLASMA KEY PARAMETERS AT AND OUT OF THERMAL EQUILIBRIUM

A. Theoretical model

By considering one electron inside a given electromagnetic environment (depicted by electric field E), one can obtain from the Newton's second law:

$$m_e \frac{dv}{dt} = -eE - k\, m_e v, \tag{1}$$

where $-k\, m_e v$ is a restoring force, v is the velocity of electron, and m_e and e are respectively mass and elementary charge of electron. Assuming the electric field as $\underline{E} = E_0 e^{i\omega t}$ and neglecting dipole creation inside plasma resolving (1), the celerity of electrons is obtained:

$$v = \frac{eE_0}{k+i\omega}\frac{1}{m_e} e^{i\omega t}. \tag{2}$$

Introducing the drift velocity one can obtain when $\omega = 0$ the parameter equal to the collision frequency υ_{e_p} of electrons with the other particles inside the plasma. So the real current density can be written as:

$$\overrightarrow{J_e} = -\frac{n_e e}{m_e}\left(\frac{-e\vec{E}_0}{\nu_{e_p+i\omega}}\right) e^{i\omega t}. \tag{3}$$

Introducing effective current inside Ampere's law we obtain:

$$\vec{\nabla} \times \vec{\mathrm{H}} = \varepsilon_0 \frac{\partial \vec{E}}{\partial t} + \overrightarrow{J_e} = \varepsilon \frac{\partial \vec{E}}{\partial t}. \tag{4}$$

Then the real permittivity is written as:

$$\varepsilon = \varepsilon_0 \left(1 - \frac{\omega_p^2}{\omega(\omega - i\,\upsilon_{e_p})}\right). \tag{5}$$

This permittivity is available for isotropic and non-magnetized plasma. We can feature key parameters: plasma pulsation $\omega_p = 2\pi f_p$ and collision frequency υ_{e_p} of electrons, and the thermal velocity of electrons. This last parameter will be given in the following, jointly

with plasma characteristic parameters (i.e., f_p and υ_{e_p}) taking into account in an original way the physical properties of plasma material.

B. Plasma characteristics and equivalent complex permittivity

Figure 3 shows frequency collisions of electrons and plasma frequency extracted from air composition and thermal assumptions (see Figs. 1-2). From equation (5), we can deduce that the formulation depends greatly on plasma state and wave frequency.

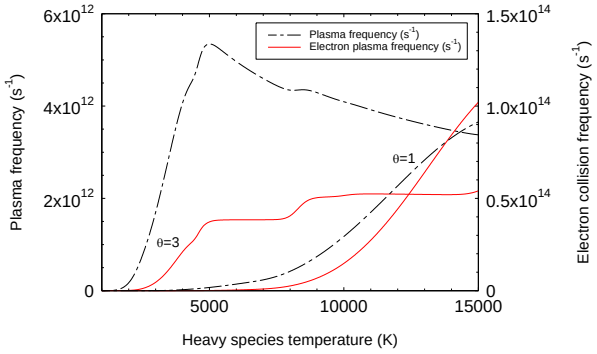

Fig. 3. Plasma frequency and electrons collisions frequency in air plasma at atmospheric pressure.

As a matter of fact, as we can see in Fig. 3, the electron plasma frequency is restricted for weaker temperatures. As a first approximation, plasma can be considered as a dielectric material. In Figs. 4-5, we have plotted the real and imaginary part of the relative permittivity for the air plasma at and out of thermal equilibrium. It is to be noted (data not shown here) that, for the lower temperature the real relative permittivity is close to 1 and the imaginary part is close to zero. Figures 4 and 5 show real components of dielectric constant are lower than unit (T_h = 10,000 K).

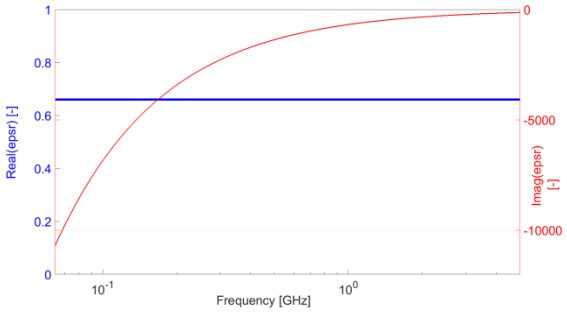

Fig. 4. Complex permittivity of the air plasma at thermal equilibrium (θ = 1): real (blue) and imaginary (red) parts at T_h = 10,000 K from 64 MHz to 5 GHz.

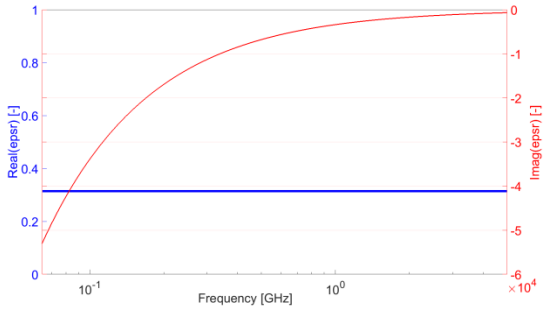

Fig. 5. Complex permittivity of the air plasma out of thermal equilibrium (θ = 3): real (blue) and imaginary (red) parts at T_h = 10,000 K from 64 MHz to 5 GHz.

III. NUMERICAL RESULTS: PLASMA CHARACTERIZATION FOR SHIELDING EFFECTIVENESS (SE) APPLICATIONS

Some EM simulations were achieved using CST© MWS to assess EM field penetration inside air plasma at and out of thermal equilibrium. Time solver and dispersive model based upon data from Fig. 3 were used to quantify plasma shielding strength (i.e., E-field magnitude decreasing while penetrating plasma material) up to 5 GHz. For the sake of exhaustiveness, the next sections will detail numerical simulations.

A. Test case #1: Assessment of canonical shielding effectiveness (SE)

The first test case is inspired from Zheng et al. works [5]. Indeed, we would like to characterize the influence of plasma physical key parameters (plasma frequency, electron collision frequency, permittivity) on electromagnetic wave (EMW) propagation in to a slab. The physical key parameters depends grandly on the chemical concentrations has can be seen by comparing the Fig. 3 with Figs. 1 and 2. The crucial part of the work relies on the characterization of material throughout models and plasma key parameters (i.e., plasma frequency f_p, and collision frequency υ_{e_p}) as depicted in Fig. 3. Those characteristics are highly dependent to the thermal equilibrium through the chemical composition.

The aims of this section are to demonstrate the difference that may be expected from taking into account (or not) potential thermal non-equilibrium jointly with the relevance of using computational electromagnetics tool (e.g., CST© with time domain solver). First of all, we put the focus on a canonical case, and in order to prepare numerical experiments in Section III.2 (test case #2), we propose to model two kinds of plasmas (data given in Fig. 3) for T_h = 10,000 K and T_h = 15,000 K with CST© MWS at thermal and non-thermal equilibrium.

Figure 6 depicts the numerical setup proposed for

straightforward characterization of the EM attenuation of waves throughout plasma illuminated by a normal-incidence plane wave. The plasma slab is a 2x2x1 cm^3 volume (Fig. 6). The time simulation (CST© MWS, time solver) is maintained up to ensure at least that more than 40 dB of the maximum energy has vanished from the computational domain. The plasma dielectric dispersion relies on purely dispersive modelling according to data in Figs. 4-5.

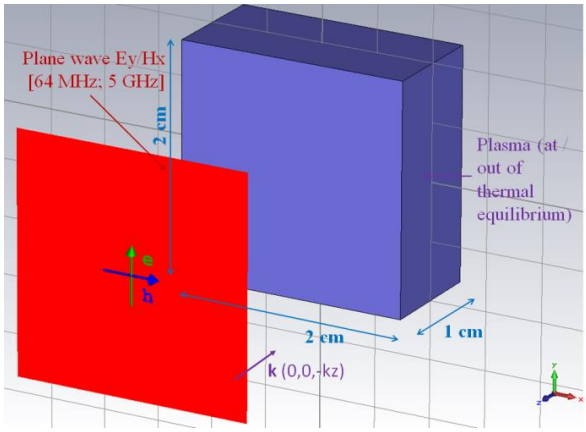

.

Fig. 6. Numerical setup for plane wave impinging on plasma slab (2 x 2 x 1cm^3, infinitely extended in x- and y-directions) using CST© MWS time solver and plasma material modelling (dispersive one).

A huge number of potential EM applications of plasma layers exist in literature as expressed in the introduction. Canonical characterization of plasma attenuation at atmospheric pressure is carried out, for example, in [15] whereas spacecraft flight re-entry is studied in [5]. In each of the two previous cases, attenuation is defined in a different manner. We will next consider the shielding effectiveness (SE) of the plasma (Fig. 9) as follows:

$$SE = \frac{incident\ EMW}{transmitted\ EMW}, \quad (6)$$

$$SE_{dB} = -20log\frac{E_{in}}{E_{out}}, \quad (7)$$

where E_{in} is the electric field located behind the infinite plasma slab (transmitted electromagnetic wave, EMW), and E_{out} is the incident EMW.

In the following and based upon relations (6-7), the transmitted electric field (E_{in}) is computed from CST© time domain solver and dispersive medium given by original theoretical models from Section II. The numerical results are compared to the analytical approach from [5] where the transmission coefficient t (t=E_{in}/E_{out} in relation (7)) is obtained as follows:

$$t = \frac{2\sqrt{\varepsilon_r}e^{ik_0 d}}{2\sqrt{\varepsilon_r}cosh(ik_p d)+(\varepsilon_r+1)sinh(ik_p d)}, \quad (8)$$

where ε_r is the complex permittivity of plasma, k_0 is the wave number in bulk medium (air), k_p is the wave number in plasma (here with different characteristics in terms of temperature, thermal equilibrium…), and d is the width of considered plasma slab.

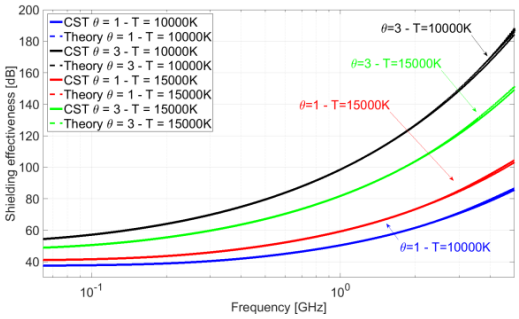

Fig. 7. Shielding effectiveness (attenuation in dB from 64 MHz to 5 GHz) at thermal equilibrium θ=1 (blue, T_h = 10,000 K; red, T_h = 15,000 K) and out of thermal equilibrium θ=3 (black, T_h = 10,000 K; green T_h = 15,000 K) relying on analytical formulation (dotted lines: reference [5]; dielectric permittivity from Figs. 4 and 5) and CST© (plain lines).

Figure 7 illustrates the impact of non-thermal equilibrium of air plasma at atmospheric pressure and at T_h = 10,000 K / T_h = 15,000 K on material SE in function of frequency; similarly to Figs. 4-5, the dielectric properties of plasma are obtained at T_h = 15,000 K (data not shown here) with original works based upon assessment of plasma characteristics from air plasma composition (Figs. 1-2). The obtained results are in accordance with the results of other authors [5, 15]. Indeed, assuming similar characteristics of plasma (e.g., pressure, heavy species distribution, width of plasma slab), tens dB of attenuation are expected in [5, 15]. We remark that electron collision frequency play major roles, their increase leading to a proportional decrease of transmitted electric fields. Consequently, the physical parameters need for EM modelling depend on plasma composition (Figs. 1 and 2.) The maximum gap existing between SE at and out of thermal equilibrium is higher for T_h = 10,000 K than for T_h = 15,000 K. Indeed, the gap is comprised between 3 dB and 45 dB considering heavy species temperature T_h = 15,000 K, whereas SE is between 5 dB and 100 dB higher out of thermal equilibrium than at thermal equilibrium at temperature T_h = 10,000 K. Finally, it is noted that the SE differences between θ=3 and θ=1 increases with frequency for each plasma temperature. By comparing our results with analytical formulation (8), Fig. 7 validates the use of fully dispersive plasma model obtained from the theoretical model proposed in this work (Section II). The next section will illustrate the importance of a careful definition of plasma characteristics (via complex permittivity and plasma characteristic frequencies) in

EMC framework.

B. Test case #2: Cabinet shielding at and out of thermal equilibrium

Relying on previous results for canonical case (test case #1), we illustrate the influence of thermal or non-thermal equilibrium assumption throughout an EMC shielding example. The numerical configuration is illustrated in Fig. 8: a perfectly conducting (PEC) enclosure (6 x 6 x 3.96 cm^3) is considered jointly with a square aperture (length=4 cm) and 4 mm-walls (and 4mm-width of plasma). Figure 8 shows the direction of the impinging plane wave (incident electric field *Ey* = 260 kV/m). Plasma characteristics are based upon results given in Figs. 4-5 (T_h = 10,000 K). Unlike the work of [16], we have to precise that the plasma is produced independently of the impinging plane. Furthermore, here we do not want to study the breaking electrical field produced by an impinging plane wave since the presence pf plasma is assumed. We will discuss the non-linear nature of plasma characteristics latter in this section.

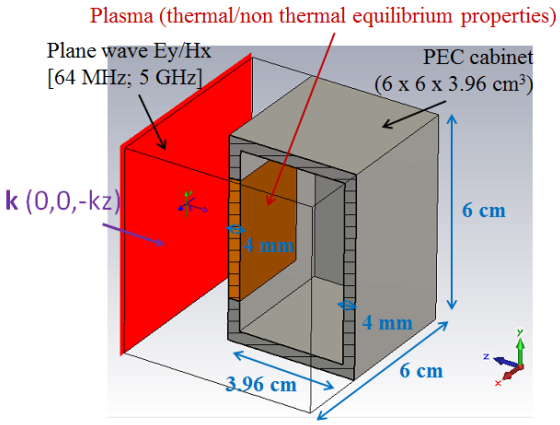

Fig. 8. Characterization of the influence of thermal (θ=1) or non-thermal (θ=3) equilibrium (numerical setup) on the SE of PEC cabinet (sectional view) subject to plane wave illumination.

Figure 9 represents the evolution of the SE of the cabinet in relation with frequency [0.064 MHz; 5 GHz]. The averaged gap existing between plasma at thermal (red) and non-thermal (green) equilibrium is between 9 dB and 45 dB. It is to be noticed that, due to the proposed configuration (worst case regarding size of the aperture and plane wave source), the shielding effectiveness without plasma material quickly decrease within negative levels (i.e., field enhancement instead of shielding) from 2.8 GHz. Contrary to previous case, the plasma slab improves SE of the system (enclosure + plasma) up to 45 dB (θ=1) and 85 dB (θ=3). It should also be noticed that the system is subject to cavity resonances, decreasing SE for instance at f=4.859 GHz (resonance frequency in accordance with inner sizes of the enclosure). Finally, due to dispersive effect, plasma slab closes the cabinet and involve enhancement of 4.859 GHz-resonance frequency as depicted in Fig. 9.

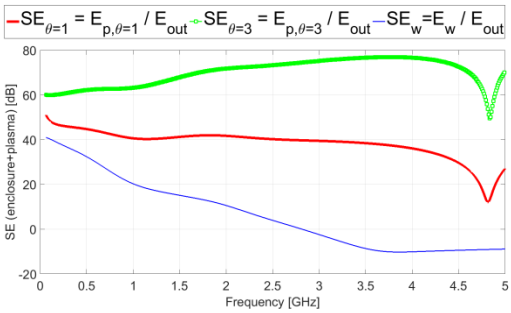

Fig. 9. SE of the cabinet (electric field measured at the center of the enclosure, Fig. 8) with plasma at (red)/out of (green) thermal equilibrium, and without plasma (blue, E_w) including only the enclosure. Results are given by normalizing data following relation (7) with E_{out}.

In order to illustrate the importance of taking into account inner thermal characteristics of plasma (differences between electrons and heavy species temperatures), it is proposed to focus on the influence of plasma by normalizing SE (Fig. 9) obtained in the two cases (θ=1) and (θ=3) by results computed without plasma material. Figure 10 shows the plasma attenuation (based upon electric field *Ey*-component computing) following the respective dB-differences $20log10(E_{\theta=1}/E_{out})$ and $20log10(E_{\theta=3}/E_{out})$ (see Fig. 9). As expected the cabinet is involved for a noticeable part in shielding characteristics. Figure 10 gives an overview of the dedicated effect of plasma material in the proposed EMC configuration (Fig. 8) by normalizing with test case involving only the enclosure. This lays emphasis on the importance of considering thermal equilibrium or not from theoretical model to EMC application since high gaps exist (from 10 dB to 40 dB) over the whole frequency bandwidth. As aforementioned in Fig. 9 and due to the characteristics of starting resonance frequency (i.e., the presence of the air aperture, see Fig. 8, involving both the resonance mode vanishing and a huge reflection of impinging plane wave), the shielding effectiveness is considerably spoiled in 'empty' case (without plasma, see blue line in Fig. 9). Contrary to previous case, plasma plays dual role since it affects the levels of fields penetrating in the cabinet but also closes it, enhancing first resonance mode influence around 4.859 GHz as illustrated in Fig. 9.

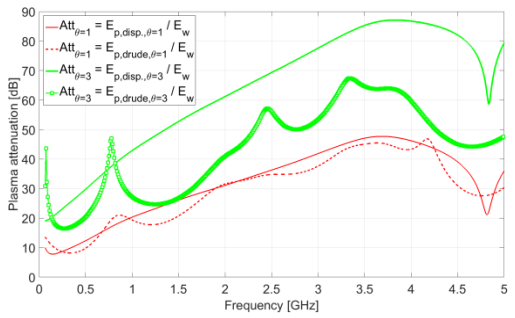

Fig. 10. Plasma attenuation including the effect of the enclosure (normalization with E-field given without plasma, E_w) at (red) and out of (green) thermal equilibrium; results are proposed including dispersive plasma medium (plain lines, see relation (5) and Figs. 4 and 5) and Drude's model (dotted lines and markers) based upon plasma characteristics (Fig. 3).

A sufficient radiation level of impinging wave in air at low temperature can enhanced an electrical breakdown. The value of breakdown electrical field depends on the air pressure, hygrometry, the cavity shape. Furthermore the nature of plasma, that vary with time, strongly depends on the shape and the power of impinging wave. Similarly to Fig. 9, Fig. 10 illustrates previous point and enriches the discussion by providing data obtained with time simulations taking into account the non-linear nature of plasma characteristics via Drude's modelling [11]. Indeed, in that case, the definition of plasma dielectric properties relies on intrinsic plasma characteristics (Fig. 3) jointly with a non-linear E-field threshold breakdown modelling as explained in the following. By varying the plasma density within a given field level, plasma attenuation is decreased relatively to purely dispersive medium (see Figs. 7 and 9). It is to be noted in Fig. 10 that weak gaps exist regarding thermal equilibrium (θ=1, red curves); huger differences are obtained out of thermal equilibrium (θ=3, green curves). The same trends between dispersive and Drude's material are observed in Fig. 10 for θ=1 (red) whereas up to 35 dB-gaps are computed for θ=3 (green). These variations mostly depend on Drude's model including: plasma characteristics (e.g., plasma frequency f_p and collision frequency υ_{e_p} from developments in Section II, here see Fig. 3 and temperature T_h = 10,000 K), and electric field breakdown level (we approximate breakdown electrical field by a constant value E_{break} = 100 kV/m). As aforementioned in [6], plasma induced by microwave may efficiently offer EMC advantages by providing interesting EM shielding properties. Indeed, when overcoming E_{break}-threshold, the plasma barrier appears as a highly conductive dielectric material. In this case, we demonstrate the capability of time domain simulations (including Drude's modelling and breakdown level) to enrich purely dispersive approach. This also lays emphasis on the huge importance of properly defining plasma characteristics (plasma frequencies and/or complex permittivity) in EMC context, especially when thermal equilibrium assumption is not satisfied. It should be noticed that, for air plasma at atmospheric pressure, purely dispersive plasma modelling is sufficient to accurately assess the EM shielding properties of the material. In this framework, plasma characterization may be useful to improve the assessment of EMC shielding.

IV. CONCLUSION AND PROSPECTS

This contribution aims at demonstrating the importance of modelling plasma behaviour in EMC framework. In this context, a particular care needs to be taken in order to properly define the impact of the physical conditions assumed for the definition of plasma. Of course, it is well-known that the composition, temperature, pressure of the material (plasma) is of great importance. The thermal equilibrium respectively between the temperatures of electrons and heavy species plays also a key role as illustrated by the different characteristics of plasma (i.e., plasma and collision frequencies) given at and out of thermal equilibrium. Obviously, this involves major changes regarding the dielectric properties of the material (complex permittivity; non-thermal equilibrium may lead to increase dielectric losses up to a scaling factor of 6 in comparison with thermal equilibrium assumption).

In this paper, we have shown the influence of the plasma thermodynamic state on the shielding properties in EMC context. At thermal equilibrium, we have observed comparable levels of electromagnetic attenuation than results found in literature. On the contrary, non-thermal equilibrium may involve noticeable increase in attenuation (here 40 dB at maximum). Using "Full-Wave" simulation tool such as CST© jointly with the proposed theoretical plasma models upgrade the physical understanding of wave propagation in complex media. Moreover, the assessment of EMC criteria (e.g., shielding effectiveness) is improved.

Further works are nowadays under consideration to enhance this study. Parametric and multi-physics works based upon these models may be useful for EMC applications and/or various electromagnetic issues (e.g., material characterization, plasma, lightning, transport, space re-entry, and communications). It should also be useful to assess the effect of non-linear field behaviour due to plasma inclusion. Based upon proposed work, it should be noticed that plasma material may be modelled throughout use of proposed plasma frequency and collision frequency (parallel to complex permittivity). This may lead to enrich time domain model and illustrates threshold effects in EMC context (involving shielding or field enhancement) and offers an extension

to multi-physics issues (e.g., electromagnetic and thermal ones).

REFERENCES

[1] S. Alavi, T. Khayamian, and J. Mostaghimi, "Conical torch: The next-generation inductively coupled plasma source for spectrochemical analysis," *Analytical Chemistry*, vol. 90, p. 3036, December 2017.

[2] N. Derkaoui, C. Rond, T. Gries, G. Henrion, and A. Gicquel, "Determining electron temperature and electron density in moderate pressure H2/CH4 microwave plasma," *J. Phys. D: Appl. Phys*., vol. 47, p. 205201, May 2014.

[3] X. Pu, Y. Cai, Y. Shi, J. Wang, L. Gu, J. Tian, and W. Li, "Diesel particulate filter (DPF) regeneration using non-thermal plasma induced by dielectric barrier discharge," *Journal of the Energy Institute*, vol. 91, pp. 655-667, June 2018.

[4] R. Brandenburg, "Dielectric barrier discharges: progress on plasma sources and on the understanding of regimes and single filaments," *Plasma Sources Sci. Technol*., vol. 26, p. 053001, July 2017.

[5] L. Zheng, Q. Zhao, and X. J. Xing, "Effect of plasma on electromagnetic wave propagation and THz communications for reentry flight," *ACES Journal*, vol. 30, no. 11, November 2015.

[6] M. Backstrom, U. Jordan, D. Andersson, A. V. Kim, M. Lisak, and O. Lunden, "Can intentional electrical discharges be used for HPM protection?," *IEEE Int. Symp. on EMC*, pp. 14-19, August 2011.

[7] A. Hamiaz, R. Klein, X. Ferrieres, O. Pascal, and J. P. Boeuf, "Modelization of plasma breakdown by using finite volume time domain method," *in Proc. 27th Annual Review in Applied Computational Electromagnetics*, Williamsburg, VA, USA, March 2011.

[8] P. André, Y. A. Barinov, G. Faure, and S. M. Shkol'nik, "Characteristics of discharge with liquid non-metallic cathode burning in air flow," *J. Phys. D: Appl. Phys*., vol. 51, 445202, September 2018.

[9] P. André and M. Abbaoui, "Déséquilibre thermique dans un plasma d'air ensemencé d'aluminium (in French)," *JITIPEE*, vol. 3, no. 2, 3, 2017.

[10] H. Li, Y. Liu, Y.-R. Zhang, F. Gao, and Y.-N. Wang, "Nonlocal electron kinetics and spatial transport in radio-frequency two-chamber inductively coupled plasmas with argon discharges," *Journal of Applied Physics*, vol. 121, p. 233302, June 2017.

[11] C. Durochat, S. Lanteri, R. Léger, C. Scheid, and J. Viquerat, "Modélisation numérique de la propagation des ondes EM en nanophotonique: une approche de GD en domaine temporel (in French)," *in Proc. Int. Symp. on EMC, CEM 2014*, Clermont-Ferrand, France, July 2014.

[12] P. André, G. Faure, S. Lalléchère, and A. Mahfouf, "Influence of the electric field and magnetic field on Debye length, London length and Kelvin length," *in Proc. Int. Symp. On EMC, CEM 2014*, Clermont-Ferrand, France, July 2014.

[13] P. André, M. Abbaoui, R. Bessege, and A. Lefort, "Comparison between Gibbs energy minimization and the mass action law for a law multitemperature plasma with application to nitrogen," *Plasma Chem. and Plasma Process*., vol. 17, no.°2, pp. 207-217, 1997.

[14] P. André, "Partition functions and concentrations in plasmas out of thermal equilibrium," *IEEE Transactions on Plasma Science*, vol. 23, no. 3, pp. 453-458, 1995.

[15] M. Laroussi and W. T. Anderson, "Attenuation of electromagnetic waves by a plasma layer at atmospheric pressure," *Int. Jour. of Infrared and Millimeter Waves*, vol. 19, no. 3, 1998.

[16] M. Talaat, M. A. Farahat, and T. Said, "Numerical investigation of the optimal characteristics of a transverse layer of dielectric barrier in a non-uniform electric field," *Journal of Physics and Chemistry of Solids*, vol. 121, pp. 27-35, October 2018.

Pascal André received a Ph.D. degree in Plasma Physics from the Blaise Pascal University in 1995. He is the author or co-author of more than 70 papers in the domain of thermal plasma physics. At the present time, he is a Full Professor at the Clermont-Auvergne University and Editor of the French journal JITIPEE (Journal International de Technologie, de l'Innovation, de la Physique, de l'Energie et de l'Environnement). His interests involve plasma out of thermodynamic equilibrium included in industrial purposes such as fuses, circuit breakers, lighting strikes at the physical laboratory of Clermont.

Géraldine Faure received a Ph.D. degree in Plasma Physics from University Blaise Pascal, Clermont-Ferrand in 1997. She is working at the physical laboratory of Clermont. Her research interests cover the fields of thermal plasmas, air and air-water plasma, atomic and molecular emission.

Ali Mahfouf received Ph.D. degree in the Domain of Thermal Plasma Physic working at the Clermont-Ferrand University in 2016. His research is focused on new approach to calculate numerically the classical transport collision integrals.

Sébastien Lalléchère received the M.Sc. and Ph.D. degrees in Computational Modeling and Electronics/ Electromagnetics from Polytech Clermont and Université Blaise Pascal (UBP), Clermont-Ferrand, France, in 2002 and 2006. He served as a Research Engineer in LASMEA, Clermont-Ferrand, France, in 2007 focusing on intensive computational methods for electromagnetics. He is currently an Associate Professor at Université Clermont Auvergne and Institut Pascal, Clermont-Ferrand, France. His research interests cover the fields of EMC including antennas and propagation, complex media, computational electromagnetics, stochastic modeling and sensitivity analysis in electrical engineering.